

Array of Multichroic Double-Slot Antennas with Cold-Electron Bolometers for the 220/240 GHz channels of the LSPE Instrument

L.S. Kuzmin, A.V. Chiginev, D.A. Pimanov, A.V. Gordeeva, S. Masi and P. de Bernardis

Abstract—The present paper tells about developing narrowband antennas for frequencies 220 and 240 GHz, which will be used in the LSPE balloon telescope to estimate foreground cosmic dust. For this goal, we used double-slot antenna with coplanar lines and Cold-Electron bolometers. The simulations show that we have achieved 5% bandwidth for 220 GHz and 5.5% bandwidth for 240 GHz for the single cell. There are also results for an array of unit cells using double-slot antennas and coplanar lines with CEBs. Besides that, the paper addresses the question of the use of SQUID readout for cold-electron bolometers.

Index Terms—CMB, LSPE, B-mode, SQUID, Cold-Electron Bolometer, coplanar lines, double-slot antenna, narrowband.

I. INTRODUCTION

LSPE is project of a balloon-borne telescope, which is developed for observation of the circular B-mode of CMB [1]. In particular, in this project it is planned to make two frequency channels on 220 and 240 GHz, which are needed to remove the influence of the cosmic dust. The special requirement for these channels is a very narrow bandwidth, which should be equal to 5% of the operating frequency.

The whole construction of the receiving system implies the use of a back-to-back horn, which acts as an element responsible for radiation diagram of the receiver. We suggest placing a planar array of the cold-electron bolometers (CEB) [2-5] and slot antennas under the back of the horn; so that the radiation diagrams of the slot antennas themselves will not affect beam characteristics of the receiver.

The best way for accurate comparison of two neighbour narrowband signals is to develop a multichroic pixel with nanofilter on chip. The first realization of nanofilter was invention of CEB with kinetic inductance of NbN strip [6]. The resonance was realized by capacitance of SIN tunnel junction and the kinetic inductance of NbN strip embedded into a cross

slot antenna. The solution of this problem is based on the use of the kinetic inductance of the superconductor, allowing to reduce linear size of such an inductor up to 300 times compared to the geometrical inductor of the same inductance. This strip is unified with CEB and called resonant cold-electron bolometer (RCEB).

The RCEB for multichroic pixels with an internal resonance by a kinetic inductance of the NbN nanostrip and a capacitance of the SIN tunnel junctions has been realized using a single Lambda slot with two RCEBs for 75 and 105 GHz [7]. However, the fabrication of kinetic inductance meets serious technological difficulties.

In the present paper, we suggest an alternative solution for creating multichroic system using internal resonance of slot antenna and capacitance of CEB.

II. SINGLE CELL FOR THE DOUBLE-SLOT ANTENNA WITH FOLDED COPLANAR LINES AND CEBs

The problem of creation of narrowband antenna is not so trivial, it requires some specific methods.

As an inductive element of a resonant circuit for matching with the capacitance of CEB, we suggest the use of the reactance of the “slot antenna + coplanar line” system. This approach implies that the imaginary part of the impedance of this reactance is positive at the operation frequency, which corresponds to the inductive character of such a system.

As the prototype of the receiving system we have chosen a CoRE two-frequency single pixel at 75 and 105 GHz. This pixel is based on the two-frequency seashell antenna, which consists of pair of slot antennas connected with CEB by coplanar lines [8-9].

However, for this antenna, we chose double-slot design with central feeding, which is done by coplanar lines, they also act as waveguides. These coplanar lines are connected to a radiation detector with low resistance, which should provide the

The work is supported by the Ministry of Education and Science of Russian Federation (Project 16.2562.2017/PCh).

L.S. Kuzmin is with Chalmers University of Technology, Gothenburg SE-41296, Sweden and also with Nizhny Novgorod State Technical University n.a. R.E. Alekseev, Minin St., 24, Nizhny Novgorod 603950, Russia (e-mail: kuzmin@chalmers.se).

A.V. Chiginev is with Nizhny Novgorod State Technical University n.a. R.E. Alekseev, Minin St., 24, Nizhny Novgorod 603950, Russia and also with Institute for Physics of Microstructures, Russian Academy of Sciences, GSP-105, Nizhny Novgorod, 603950, Russia (e-mail: chig@ipmras.ru).

D.A. Pimanov is with Nizhny Novgorod State Technical University n.a. R.E. Alekseev, Minin St., 24, Nizhny Novgorod 603950, Russia (e-mail: macpimanov@gmail.com).

A.V. Gordeeva is with Nizhny Novgorod State Technical University n.a. R.E. Alekseev, Minin St., 24, Nizhny Novgorod 603950, Russia (e-mail: a.gordeeva@nntu.ru).

S. Masi is with Dipartimento di Fisica, Università La Sapienza, P. le A. Moro 2, I-00185 Roma, Italy (e-mail: silvia.masi@roma1.infn.it)

P. de Bernardis is with Dipartimento di Fisica, Università La Sapienza, P. le A. Moro 2, I-00185 Roma, Italy (e-mail: paolo.debernardis@roma1.infn.it)

required frequency characteristics for narrowband antenna. As a detector of microwave radiation, we suggest to use a CEB. It has many advantages compared with other types of bolometers. The most important of them are their unique sensitivity, wide dynamic range due to electron cooling, and the insensitivity to cosmic rays [5]. A schematic view of CEB and its energy diagram are shown in Fig. 1a and Fig. 1b respectively.

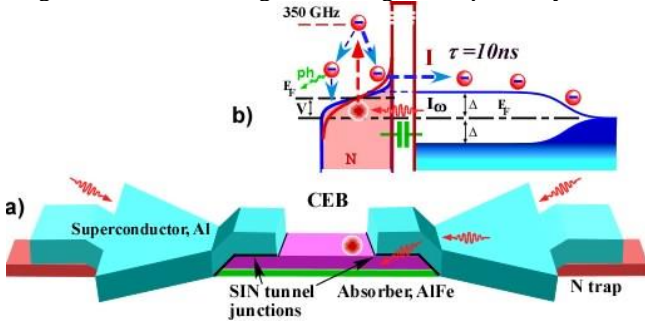
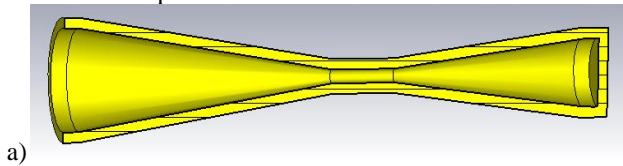


Fig. 1. (a) A schematic view of CEB; (b) energetic diagram of CEB.

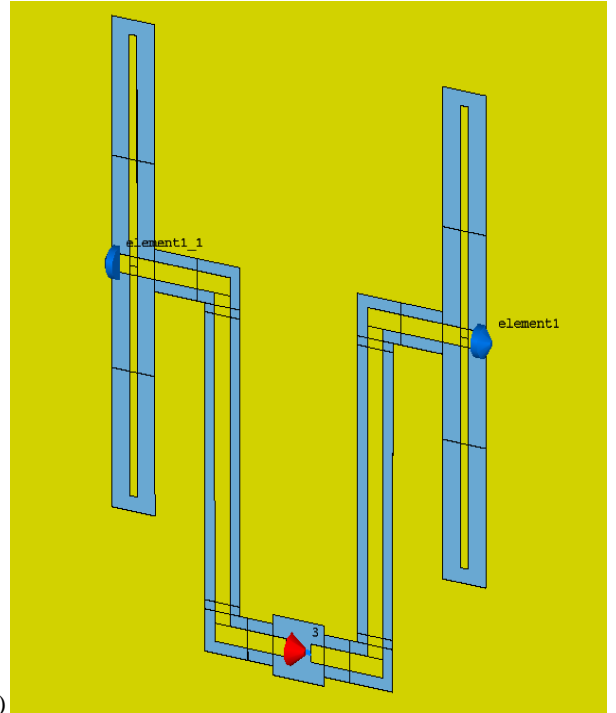
Also, this antenna will be used with a back-to-back feedhorn. It makes the radiation diagrams of antenna slots not affecting the beam characteristics at the receiver. The design of feedhorn is shown in Fig. 2a.

The design for single cell of double-slot antenna is presented in Fig. 2b. The antenna consists of two resonant slots and a coplanar line, which is folded to acquire better frequency band characteristics. The coplanar lines length for each frequency was set to get the needed working frequency. The distance between antenna slots was chosen after a number of simulations in CST Microwave Studio. In total, these parameters let us obtain the required frequency characteristics. CEB is put into the gap in the central wire of the coplanar line. The position of CEB is shown as a red triangle in Fig. 2b.

For CEB, the DC biasing is provided through coplanar lines by DC connectors, which are located under the ground plane. Blue triangles in Fig. 2b show the positions of DC connectors. In numerical simulations, the influence of the DC connectors is modeled by lumped capacitances, which are placed between the ends of coplanar lines and the ground plane. These capacitances are set to 350 fF, which is the estimated value of DC connectors' capacitance.



a)



b)

Fig. 2. (a) Back-to-back feedhorn used for the antenna system; (b) single cell of double-slot antenna design overview in CST Microwave Studio.

Fig. 2b shows the single cell for antenna for 220 GHz. There is only one difference in antenna design for 240 GHz, the total length of central coplanar line; it is 60 μm shorter. The calculations have been performed using frequency domain solver. In electrodynamic part of simulations, these designs have shown the following values of the impedance: ReZ (220 GHz) is 6.8 Ohm, ReZ (240 GHz) is 7.7 Ohm; ImZ (220 GHz) is 36.3 Ohm, ImZ (240 GHz) is 32.9 Ohm. We will need these values for getting the required resonances at needed operating frequencies in the schematic part of the simulations.

The equivalent circuit of the antenna connected to a CEB is presented in Fig. 3. The values of R_{abs} and C_{SIN} are chosen in this way: $R_{abs} = ReZ(f_0)$, $C_{SIN} = (2\pi f_0 \cdot ImZ(f_0))^{-1}$; here $Z(f)$ is the diagonal component of the Z -matrix calculated in electrodynamic part (see above). The C_{sin} values should make the total capacitances of C_{sin} and C_e form the series resonance with L_e at frequencies 220 and 240 GHz respectively. This method of parameters choice is correct only when $ImZ(f_0) > 0$ and when $|S_{mn}(f_0)| \ll 1$, where S_{mn} are the non-diagonal components of the S -parameters matrix which is calculated in electrodynamics.

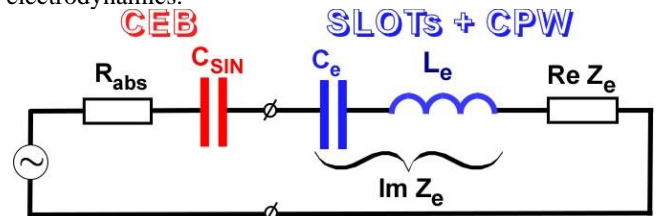


Fig. 3. Equivalent circuit of the Double-Slot antenna connected to a CEB by coplanar lines.

Fig. 4 shows the frequency characteristics of the single cell with CEB after calculations in schematics. The parameters used in schematics are following. For 220 GHz antenna, R_{abs} is 6.8

Ohm, and for 240 GHz antenna, R_{abs} is 7.7 Ohm. C_{SIN} for 220 GHz is 19.4 fF, and for 240 GHz it is 23.4 fF. These values are set to obtain the best impedance matching at operating frequencies.

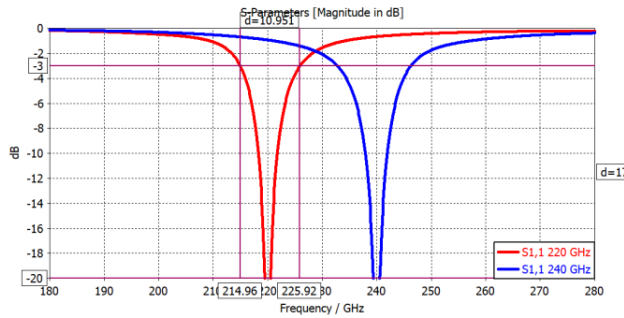


Fig. 4. Frequency characteristics of double-slot antennas with CEBs tuned to 220 GHz (red) and 240 GHz (blue) in CST MWS schematic.

As one can see in Fig. 4, the bandwidths at -3dB are even less than 11 GHz for 220 GHz and about 13.5 GHz for 240 GHz. Bandwidth for 220 GHz meets the requirements for the receiving system of LSPE well; it is 5% from operating frequency. Bandwidth for 240 GHz nearly meets the requirements for this receiving system; it is about 5.5% from operating frequency.

III. MULTI-CELL DOUBLE-SLOT ANTENNA WITH COPLANAR LINES AND CEBs

In this paragraph, we consider an array of slot antennas, which are connected in series by coplanar waveguides (CPW). The main advantage of this model is a simple single-layer technology, which means that the DC connections between CEBs are made through the same CPWs that connect the antenna cells in AC. Thus, there is no need to use separate DC connectors to feed the cells with DC bias. This solution to a greater extent simplifies the technology, but restricts the applicability of the array to the case of the current biasing of CEBs.

The single-layer slot antenna array is shown in Fig. 5. It has 45 slots for 220 GHz channel and 45 slots for 240 GHz channel on a single 3*3 mm² substrate. At this approach, the dimensions of all parts of the unit cell for 240 GHz channel are obtained from the same ones, which are set on 220 GHz channel cell by simple scaling. On the opposite side of the substrate, there is a special waveguide port, which is used as a source of the electromagnetic radiation in the numerical modelling. In the present computations, we work with the mode E_{01} .

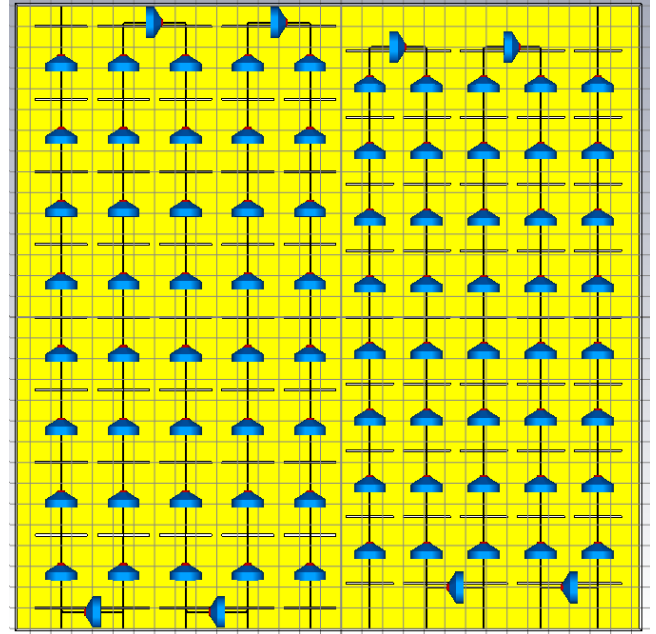


Fig. 5. The finite single-layer array of slot antennas consisting of 45 slots for 220 GHz channel (left part) and 45 slots for 240 GHz channel (right part). The blue and small red triangles denote capacitance and absorber resistance of CEB, respectively. The size of the array is 3*3 mm².

Figs. 6,7 show the power, which is accepted by all absorbers of the CEB at one frequency channel. In Fig. 6, one sees the curves for two values of absorber resistance – 10 Ohm and 17 Ohm. As we expected, the resonant curves do not shift when changing the absorber resistivity. At higher values of R the total absorption efficiency is getting higher, but the FWHM of the resonances also increases (see Table I). The decrease of R leads to corresponding decrease of the FWHM, but the absorption efficiency becomes lower.

Fig. 7 shows the accepted power for different values of SIN capacitances. We see that greater values of C lead to increase in absorption efficiency, but obviously shift the resonance frequencies towards lower values. The variations of C have only small influence on FWHM (Table I).

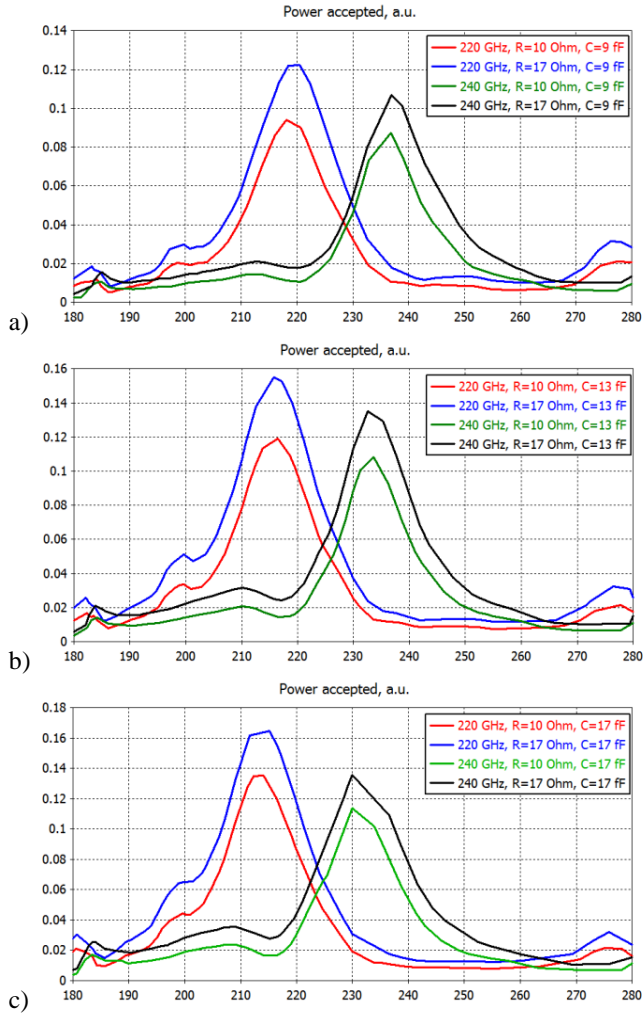


Fig. 6. Power accepted by all CEBs' absorbers, vs frequency, at a fixed CEB capacitance: (a) $C=9$ fF, (b) $C=13$ fF, (c) $C=17$ fF.

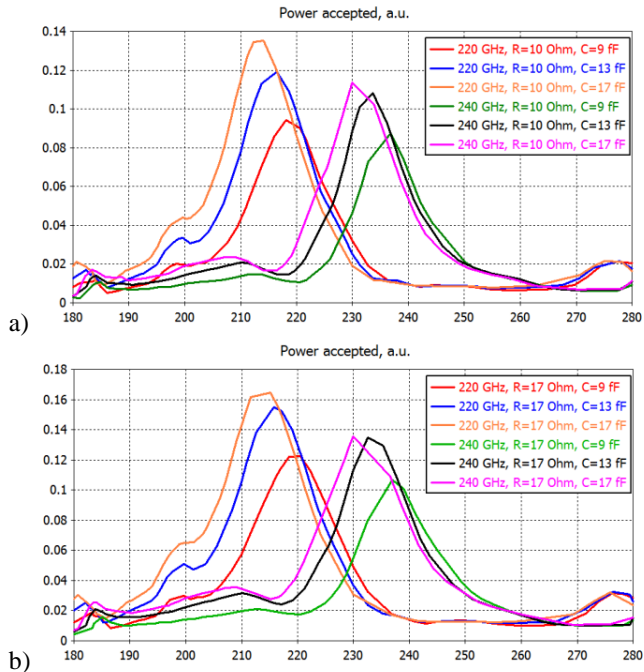


Fig. 7. Power accepted by all CEBs' absorbers, vs frequency, at a fixed absorber resistance: (a) $R=10$ Ohm, (b) $R=17$ Ohm.

TABLE I
WIDTHS OF THE RESONANT CURVES IN FIGS. 6, 7

R_0 , Ohm	C_0 , fF	220 GHz channel			240 GHz channel		
		F_{max} , GHz	FWHM		F_{max} , GHz	FWHM	
			GHz	%		GHz	%
17	9	219.59	18.19	8.28	236.99	17.54	7.4
	13	215.66	17.55	8.14	232.56	15.89	6.83
	17	215.2	18.3	8.5	230	18.4	8
10	9	218.14	16.59	7.61	236.77	13.97	5.9
	13	216.38	16.32	7.54	233.64	14.15	6.06
	17	213.28	16.4	7.69	231.67	16.1	6.95

Table I shows bandwidths for 220 and 240 GHz frequency channels. These bandwidth values are close to the requirements of 5% from central frequency, but the system needs further improvements.

IV. MATCHING OF COLD-ELECTRON BOLOMETERS WITH SQUID READ-OUT

The integration of cold-electron bolometers with the multiplexing system is an important step towards the use of CEB as detectors in modern telescopes. Multiplexing can significantly simplify the readout system, which is a significant advantage for projects with a large number of detectors. Currently, the most developed systems for multiplexing are based on SQUIDs for TES bolometers, and their use also for CEB seems to be a logical development. Therefore, in this section, we use the sensitivity of SQUIDs from TES multiplexing systems to calculate the total sensitivity of the CEB with these systems.

In Fig. 8, we present the different components of noise equivalent power (NEP) of the bolometer array, composed from 45 elementary cells from Fig. 2b. There are two NEP components coming from the bolometers itself: the electron-phonon noise (NEP_{e-ph}) and the current and heat-flow noise through SIN junctions (NEP_{SIN}), one component comes from a read-out system (NEP_{SQUID}) and one component comes from the incoming power (photon noise NEP_{ph}). The sum of the first three components is defined as bolometer NEP. The sensitivity of the SQUID array is taken from [10] and equals $3.5 \text{ pA/Hz}^{1/2}$.

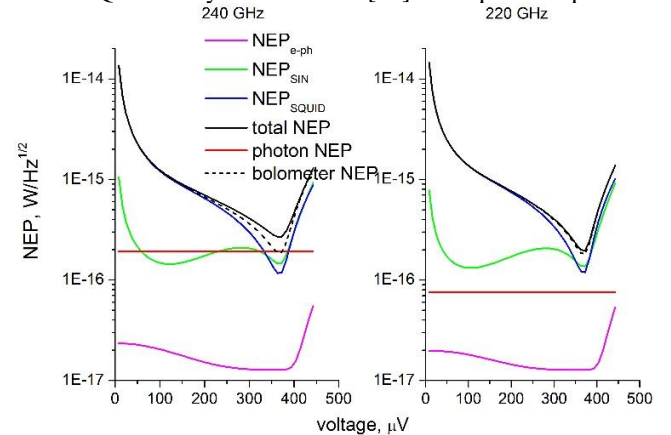


Fig. 8. NEP versus voltage of an array from 45 bolometers, connected in parallel, with SQUID read-out for 240 and 220 GHz channels.

Two channels 220 and 240 GHz have different power load 6 and 20 pW correspondingly. This power is divided between 45 bolometers in each channel.

One can see that for both channels 220 and 240 GHz there are two major NEP components: NEP_{SIN} and NEP_{SQUID} - noise of read-out electronics, which limit the sensitivity of the detector. The operation point in voltage bias mode for SQUID read-out is situated near the gap at 370 μ V, where the resistance of the bolometer array is just 5-6 Ohms. The normal resistance of a single bolometer is 600 Ohms.

The bolometer noise is less than the photon noise for 240 GHz channel at the bias point, which means the photon noise limited operation. In order to reach this mode for 220 GHz channel one can increase the SQUID sensitivity and decrease the SIN noise by decreasing the number of bolometers in the array for this channel.

Unlike TES, CEBs can receive radiation in a wide power range without experiencing saturation problems. To illustrate this, we calculated the sensitivity depending on the received power in the range from 2 to 30 pW for the 240 GHz channel (see Fig. 9).

On this graph, one can see the level of the dark noise - the bolometer noise without power load or with small power loads. For this array it is $1.2 \cdot 10^{-16}$ W/Hz^{1/2}. With increase of the power, the NEP_{ph} increases and at 13 pW becomes higher than the bolometer NEP. At this power, the photon noise limited operation starts and continues much above 30 pW, not shown here.

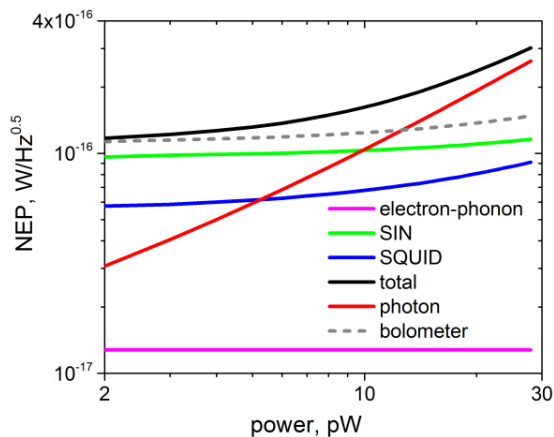


Fig. 9. NEP versus absorbed power of an array from 45 bolometers, connected in parallel, with SQUID read-out for 240 GHz channel.

Let us summarize the results of this section. The ration of the photon NEP to the bolometer NEP is $7.6 \cdot 10^{-17} / 1.2 \cdot 10^{-16} = 0.6$ for 220 GHz channel and $1.8 \cdot 10^{-17} / 1.7 \cdot 10^{-16} = 1.0$ for 240 GHz channel.

V. CONCLUSIONS

The results, acquired from numeric modelling, show that we have developed efficient designs of single cell for a double-slot antenna with folded coplanar lines, connected to CEB, for production. The results for modeled single cell for 220 GHz meet the requirements for LSPE project well. There is already going further research to create the voltage biased array of these

cells on a single substrate. The bandwidth of the single cell for 240 GHz slightly exceeds the requirements for LSPE project. So this design should be improved in terms of characteristics and used in voltage biased array too.

Also, a lot of modeling has been done for the current biased array of a various number of unit cells made of two slots with straight coplanar lines, connected to CEB. From the results, we can see that the bandwidths for this approach exceed the bandwidth requirements of 5% of operating frequencies. But they get close to the needed values. The minimal reached bandwidth at 220 GHz is 7.5% of central frequency, at 240 GHz it is 5.9%. Further research will be aimed at improving these results to meet the LSPE project requirements and to construct a single-layer antenna array with parallel connections for use with a SQUID readout.

Besides, some research was done for matching of CEBs with SQUID read-out where the possibility to use such read-out for cold electron bolometers is checked. The ration of the photon NEP to the bolometer NEP is 0.6 for 220 GHz channel and 1.0 for 240 GHz channel. Also, we can say that CEBs are photon noise limited, because the bolometer noise is less than the photon noise.

ACKNOWLEDGEMENTS

The authors would like to thank L. Lamagna, A. Sobolev and A. Pankratov for useful discussions.

REFERENCES

- [1] The LSPE collaboration 2012 *Proc. SPIE* 8446, 84467A.
- [2] Kuzmin L 2002 In: Pekola J., Ruggiero B., Silvestrini P. (eds) International Workshop On Superconducting Nano-Electronics Devices, Springer, Boston, MA, 145–154; Kuzmin L and Golubev D 2002 *Physica C* 372-376 378
- [3] Kuzmin L 2008 *Journal of Physics: Conference Series* 97 012310
- [4] Tarasov M A, Kuzmin L S, Edelman V S, Mahashabde S, de Bernardis P 2011 *IEEE Trans. on Appl. Supercond.* 21 3635.
- [5] Salatino M, de Bernardis P, Kuzmin L S, Mahashabde S., Masi S. 2014 *J. Low Temp. Phys.* 176 323
- [6] Kuzmin L S 2014, *IEEE Trans. on THz Sci. Technol.* 4 314-320
- [7] Kuzmin L S, Mukhin A S, and Chiginev A V, 2018 *IEEE Trans. on Appl. Supercond.* 28 2400304
- [8] Kuzmin L S, Chiginev A V, Matrozzova E A, Sobolev A S, 2016 *IEEE Trans. on Appl. Supercond.*, 26 2300206
- [9] L.S. Kuzmin, A.V. Blagodatkin, A.S. Mukhin, D.A. Pimanov, V.O. Zbrozhek, A.V. Gordeeva, A.L. Pankratov, A.V. Chiginev (2019), *Superconductor Science and Technology*, Volume 32, 035009.
- [10] Vaccaro D, Baldini A M, Cei F, Galli L, Grassi M, Nicolo D, Piendibene M, Tartari A, Spinella F, Signorelli G. "A frequency domain multiplexing system to readout the TES bolometers on the LSPE/SWIPE experiment," 2018 *Nuclear Inst. and Methods in Physics Research*, A936 169-171